Luo et al. Nanoscale Research Letters (2017) 12:99
DOI 10.1186/s11671-017-1864-8

Nanoscale Research Letters

NANO EXPRESS Open Access

Graphene Oxide-Polymer Composite Langmuir Films Constructed by Interfacial Thiol-Ene Photopolymerization

Xiaona Luo[1,2†], Kai Ma[2†], Tifeng Jiao[1,2,3*], Ruirui Xing[2,3], Lexin Zhang[2], Jingxin Zhou[2] and Bingbing Li[4*]

Abstract

The effective synthesis and self-assembly of graphene oxide (GO) nanocomposites are of key importance for a broad range of nanomaterial applications. In this work, a one-step chemical strategy is presented to synthesize stable GO-polymer Langmuir composite films by interfacial thiol-ene photopolymerization at room temperature, without use of any crosslinking agents and stabilizing agents. It is discovered that photopolymerization reaction between thiol groups modified GO sheets and ene in polymer molecules is critically responsible for the formation of the composite Langmuir films. The film formed by Langmuir assembly of such GO-polymer composite films shows potential to improve the mechanical and chemical properties and promotes the design of various GO-based nanocomposites. Thus, the GO-polymer composite Langmuir films synthesized by interfacial thiol-ene photopolymerization with such a straightforward and clean manner, provide new alternatives for developing chemically modified GO-based hybrid self-assembled films and nanomaterials towards a range of soft matter and graphene applications.

Keywords: Graphene oxide, Thiol-ene photopolymerization, Langmuir film, Self-assembly, Composite film

Background

Graphene oxide (GO)-based composites have received great attention over the past decade due to abundant oxygen-containing functional groups, which demonstrate GO moderate water dispersibility and reactive sites for further modification [1–4]. For examples, in recent years, Kim's group has achieved excellent research works on the investigation of chemical modification of carbon-based materials and graphene nanocomposites as well as the applications for supercapacitors and liquid crystals [5–10]. In recent years, a lot of efforts have been devoted to rational design and controlled synthesis of various GO-based organic/inorganic nanocomposites, which promises better processability with electronic, optical, and electrochemical properties as well as great developments for nanomaterial applications [11–13]. The chemical modification and functionalization of GO materials with organic compounds are needed in order to make them appropriate for good dispersion and various applications [14–16]. For example, various small molecules including long-chain alkylamine, isocyanate derivatives, porphyrin, dopamine, or tetrathiafulvalene can be utilized to modify GO to obtain good dispersed in solvent and useful optical properties [17–21]. In comparison with small molecules, polymers can be also employed to modify GO to improve the properties of GO-based composites in distinct domains. For example, poly(2-(dimethylamino) ethyl methacrylate) and poly(vinyl alcohol) have been utilized to functionalized GO with different chemical reactions [22, 23]. However, this strategy more or less suffers from GO sheet aggregation, incomplete adsorption of organic molecules, and undesired side effects, which is unfavorable for subsequent desired applications. Alternatively, click chemistry has attracted great development in recent years due to its modular nature, high selectivity, and yields [24–27]. In contrast to click chemistry for Cu(I) system [28], no catalyst is required as the reaction is initiated thermally or photochemically. It is reported that the click chemistry has been displayed to functionalize GO with the

* Correspondence: tfjiao@ysu.edu.cn; li3b@cmich.edu
†Equal contributors
[1]State Key Laboratory of Metastable Materials Science and Technology, Yanshan University, Qinhuangdao 066004, People's Republic of China
[4]Department of Chemistry and Biochemistry, Central Michigan University, Mount Pleasant, MI 48859, USA
Full list of author information is available at the end of the article

thiol-ene/thiol-yne reactions or the azide-alkyne reactions [29–32]. Hence, it remains a formidable challenge to directly synthesize GO-based composites with eco-friendly and condition-gentle process in an effective organized self-assembly manner. On the other hand, Langmuir and Langmuir-Blodgett (LB) techniques are well known as a sophisticated and effective way in organizing molecules or building blocks in a two-dimensional confined environment to obtain interfacial organized films [33–35].

Since the initial reports about GO self-assembly in Langmuir films from Huang's group [36, 37], some recent studies present the successful preparation of GO monolayer or GO-based composite films using the LB assembly method [38–46]. It can be expected that a combination of GO-based composites involved in click chemistry and self-assembly films by Langmuir technique should be particularly advantageous owing to their excellent biocompatibility, moderate nanostructures, and enhanced mechanical and chemical properties. To the best of our knowledge, GO-polymer composite films, particularly Langmuir films by interfacial thiol-ene photopolymerization, have not yet been reported and obtained. Thus, aqueous soluble poly(-ethylene glycol) diacrylate (abbreviated as DA) containing a number of ethylene glycol as molecular skeleton and ene residues as headgroups capable of donating photopolymerization has been chosen for the formation of composite films.

Herein, we report the synthesis of stable GO-polymer composite Langmuir films by in situ interfacial thiol-ene photopolymerization at room temperature (Fig. 1), without the use of any crosslinking and stabilizing agents by

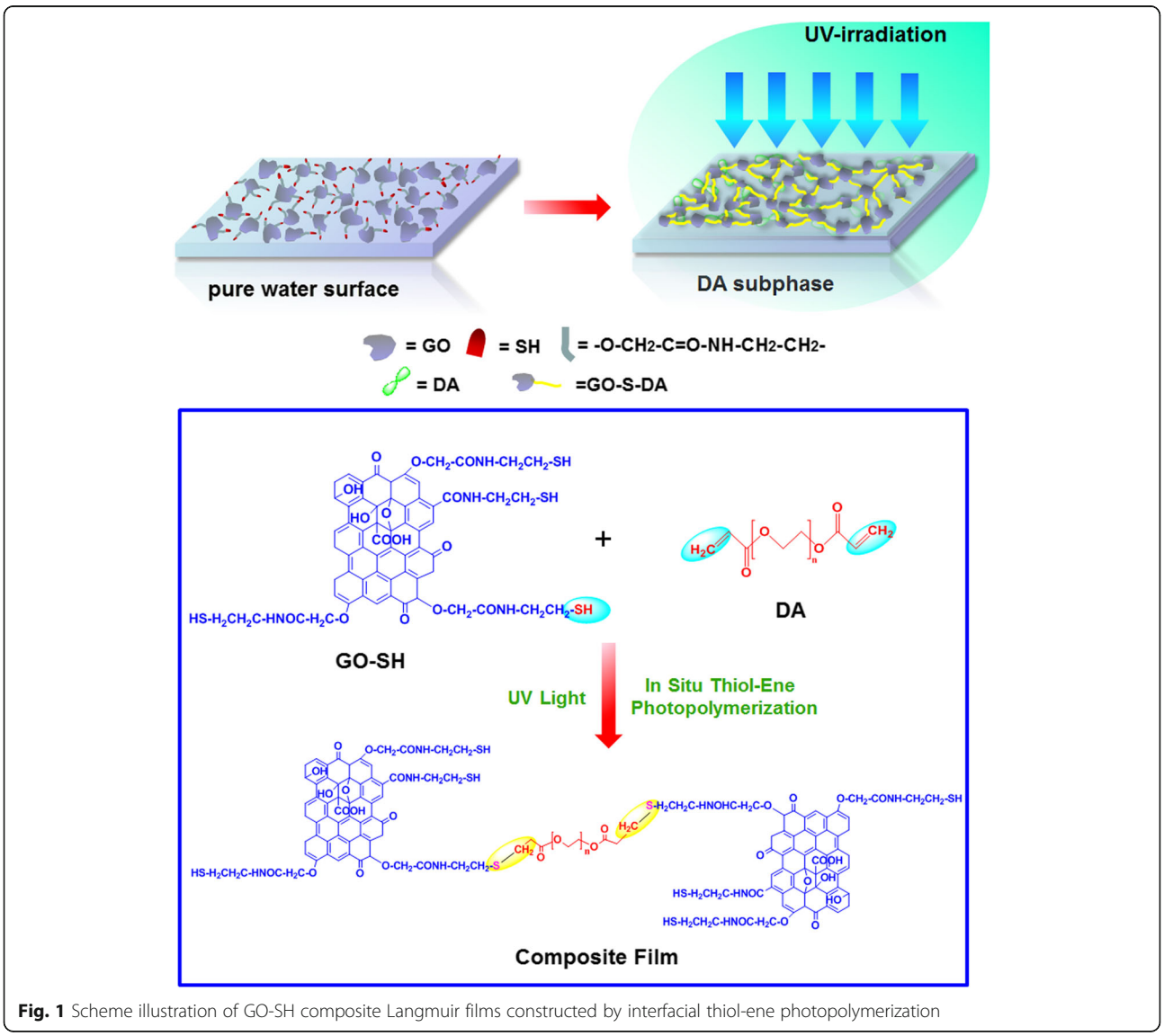

Fig. 1 Scheme illustration of GO-SH composite Langmuir films constructed by interfacial thiol-ene photopolymerization

a facile and effective manner. We discover that photopolymerization reaction between thiol groups modified GO sheets and ene in polymer molecules is responsible for formation of such kind of composite films. Also, the as-prepared films can be easily transferred onto different supported substrates with assistance of the Langmuir-Blodgett (LB) assembly technique, which show potential to enhance mechanical and chemical properties and promote excellent biocompatibility. Thus, the present GO-polymer composite Langmuir films will provide significant potential for application in soft matter engineering and GO functionalization.

Methods

The experimental used materials, poly(ethylene glycol) diacrylate (M_w = 1000 g mol^{-1}, abbreviated as DA), cysteamine (95%, abbreviated as CA), and chloroacetic acid were purchased from Aladdin Reagent (Shanghai, China). Graphite powder (325 mesh, 99%) was purchased from Alfa Aesar Chemicals (Shanghai, China). N-(3-dimethylaminopropyl)-N′-ethylcarbodiimide hydrochloride (EDC-HCl) and N-hydroxysuccinimide (NHS) were purchased from Sigma-Aldrich and were used without purification. Sulfuric acid (H_2SO_4, 98%), potassium permanganate ($KMnO_4$), potassium nitrate (KNO_3), hydrogen peroxide (H_2O_2, 30%, *w*/*w*), and hydrochloric acid (HCl) were purchased from Beijing Chemicals or Tianjin KaiTong Chemicals and used without further purification. All aqueous solutions were prepared with water purified in a double-stage Milipore Milli-Q Plus purification system. Firstly, graphene oxide (GO) was prepared from graphite powder by a modified Hummers method [47]. Then, the carboxyl-functionalized GO (named as GO–COOH) was prepared according to the reported literature [48] and freeze dried in low temperature −50 °C). Thiol functionalization was done following analogous procedure described in the literatures [49, 50] and modified as described in the following. The obtained dispersion of exfoliated GO–COOH (100.0 mL of 1.5 mg/mL) was mixed with 2.55 g of NHS and 4.28 g of EDC-HCl into a round flask, under ice bath. After stirring vigorously for 2 h, 3.0 g of CA was added to the mixture and left stirring overnight under ice bath and next 3 days at room temperature. The resulting thiol-modified GO solid (named as GO-SH) was separated by filtration by using an amide membrane filter (0.2 μm), repeatedly washed with deionized Milli-Q water. Then, the solid was dispersed with water and dialyzed in water for 4–5 days with dialysis tubing (MWCO 12400). After dialysis, GO-SH powder was obtained by freeze-drying.

The interfacial characterization and LB film transfer were carried out in KSV-NIMA Minitrough LB system. The trough was carefully cleaned with chloroform and ethanol and then filled with DI water or aqueous DA solution. After a sonication of 10 min, some volumes of GO-SH spreading solution (0.504 mg/mL, different mixed solvent ratios and volumes) were dropwise spread onto pure water surface or DA subphase solution (0.500 g/L) using a glass syringe. Surface pressure was monitored using a tensiometer attached to a Wilhelmy plate. The film was compressed by barriers at a speed of 2 mm/min. For the Langmuir film of GO-SH on DA subphase by photoreaction, UV light of 365 nm was irradiated on interfacial films at 5 min before compression begin and kept through whole compress process. The GO-SH monolayer was transferred to substrates at various points during the compression by vertically dipping the substrate into the trough and slowly pulling it up (2 mm/min). Mica, quartz, and, CaF_2, glass plates were used as the substrates to transfer monolayer or multilayer for the next morphological and spectral characterizations. Quartz and glass plates were treated with 1:1:5 NH_4OH:H_2O_2:H_2O (by volume) and washed repeatedly with deionized water before use.

The morphology of composite films were characterized by using a field-emission scanning electron microscopy (FE-SEM, S-4800II, Hitachi, Japan) with the accelerating voltage of 5–15 kV. The chemical composition of the samples was characterized by energy-dispersive X-ray spectroscopy (EDXS). EDXS analysis was typically performed at an accelerating voltage of 200 kV, using an Oxford Link-ISIS X-ray EDXS microanalysis system attached to SEM. Atomic force microscopy (AFM) images were measured by using a Nanoscope model MultiMode 8 Scanning Probe Microscope (Veeco Instrument, USA) with silicon cantilever probes. Raman spectroscopy was performed using a HORIBA Jobin Yvon XploRA PLUS confocal Raman microscope equipped with a motorized sample stage. The wavelength of the excitation laser was 532 nm, and the power of the laser was kept below 1 mW without noticeable sample heating. The intensity of a Raman peak was extracted from the maximum value after baseline subtraction over corresponding spectral range. X-ray photoelectron spectroscopy (XPS) was performed on the Thermo Scientific ESCALab 250Xi using 200 W monochromated Al Kα radiation. The 500 μm X-ray spot was used for XPS analysis. The base pressure in the analysis chamber was about 3×10^{-10} mbar. Typically, the hydrocarbon C1s line at 284.8 eV from adventitious carbon is used for energy referencing. Both survey scans and individual high-resolution scans for S(2p), O(1s), and C(1s) peaks were recorded. FTIR spectra were recorded on a Fourier infrared spectroscopy (Thermo Nicolet Corporation) by the conventional KBr disk tablet method or composite films on CaF_2 plates. X-ray diffraction study was carried out by using an X-ray diffractometer (SmartLab, Rigaku) equipped with a conventional Cu Kα X-ray radiation (λ = 1.54 Å) source and a Bragg diffraction setup. Elemental analysis was carried out with a FlashEA Carlo-Erba-1106 Thermo-Quest. A UV lamp (20 mW/cm^2,

λ = 365 nm; LUYOR-3405; LUYOR Corporation) was used to irradiate the Langmuir films to perform the photochemical reactions.

Results and Discussion

The thiol-functionalized GO-SH material can serve as building blocks for preparation of Langmuir films and subsequent in situ interfacial thiol-ene photopolymerization under UV light irradiation by standard Langmuir self-assembly technique. Figure 1 demonstrates the illustration of GO-SH composite Langmuir films constructed by in situ thiol-ene photopolymerization. For this, the precursor GO, the intermediate GO–COOH, and the final building block GO-SH were synthesized and characterized by many methods. XRD curves of as-prepared materials show the disappearance of Bragg peaks at 2θ value of 11.2° assigned to the (001) diffraction peak and presence of new broad peak at 2θ value of 22.1° for GO-SH (Additional file 1: Figure S1), which indicate successful thiolation in GO sheet and 3D structural composite formation due to thiol-functionalization [49]. The elemental analysis data (Additional file 1: Table S1) of as-prepared GO-based materials show the obvious increment of carbon composition and appearance of sulfur component with value of 10.10 ± 0.07 wt.% for obtained GO-SH. The comparison of XPS data and elemental analysis data show similar calculated N/C ratios and S/C ratios (Additional file 1: Table S2), which is almost in agreement with the above obtained results. Thus, we inspected the interfacial phase behaviors and characterized the Langmuir and the transferred LB films of GO-SH by means of morphological and spectral methods.

Firstly, we measured the surface pressure-area isotherms of as-prepared Langmuir films at room temperature (Fig. 2). The optimization of used different spreading mixed solvents and volumes for GO-SH Langmuir film spread on pure water surface was demonstrated in Fig. 2a. It show that the optimized spread condition (methanol/chloroform 2:3 (*V*/*V*), 300 μL) seem suitable for the next interfacial characterization. Then, as shown in Fig. 2b, it can be easily observed that the isotherm of GO-SH spread on pure water surface show slow increment of pressure at trough area of 77 cm^2 until reaching 18 mN/m at compression end of trough area 23 cm^2. For the GO-SH film on DA subphase without UV light irradiation, the obtained curve demonstrate increment of pressure at the beginning of compression and long platform region after 11 mN/m, suggesting possible conformation change of building block GO-SH due to the adsorption process with DA molecules in subphase solution. In addition, for the GO-SH film on DA subphase with UV light irradiation, the platform region disappears and the final surface pressure increase to the value of 28 mN/m. The obvious change in isotherms suggests the occurrence of interfacial thiol-ene photopolymerization between thiol groups in GO-SH and DA molecules with UV light irradiation and formation of composite Langmuir films.

The morphologies of the nanostructures of monolayer GO-SH Langmuir films were characterized by AFM (Fig. 3). The formed different nanostructures are obviously observed. Firstly, at low surface pressure of 5 mN/m, the thiol-functionalized GO sheet fabricate the GO-SH Langmuir films with the height distribution of 1.2 ± 0.2 nm (Fig. 3a'). When from DA subphase without UV light, films with small aggregates on surface dominate with the main height distribution of 3.4 ± 0.3 nm (Fig. 3b'), suggesting the possible interfacial adsorption of DA molecules on GO sheet due to hydrophilic force and Van der Waals force or bilayer film formation due to conformation change of GO-SH. In addition, as for the film from DA subphase with UV light, the nanostructures become cluttered in three dimensional modes

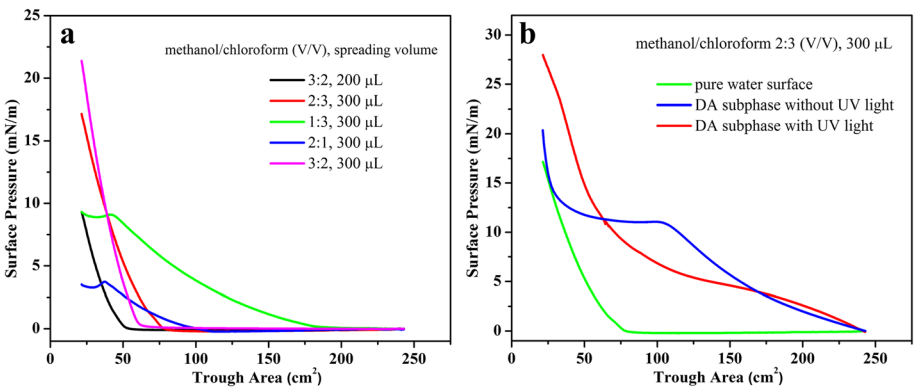

Fig. 2 Surface pressure-area isotherms of Langmuir films of as-prepared GO-SH solution: **a** pure water surface, change of different mixed solvent ratios and volumes; **b** DA subphase with/without UV light at preferred spreading condition

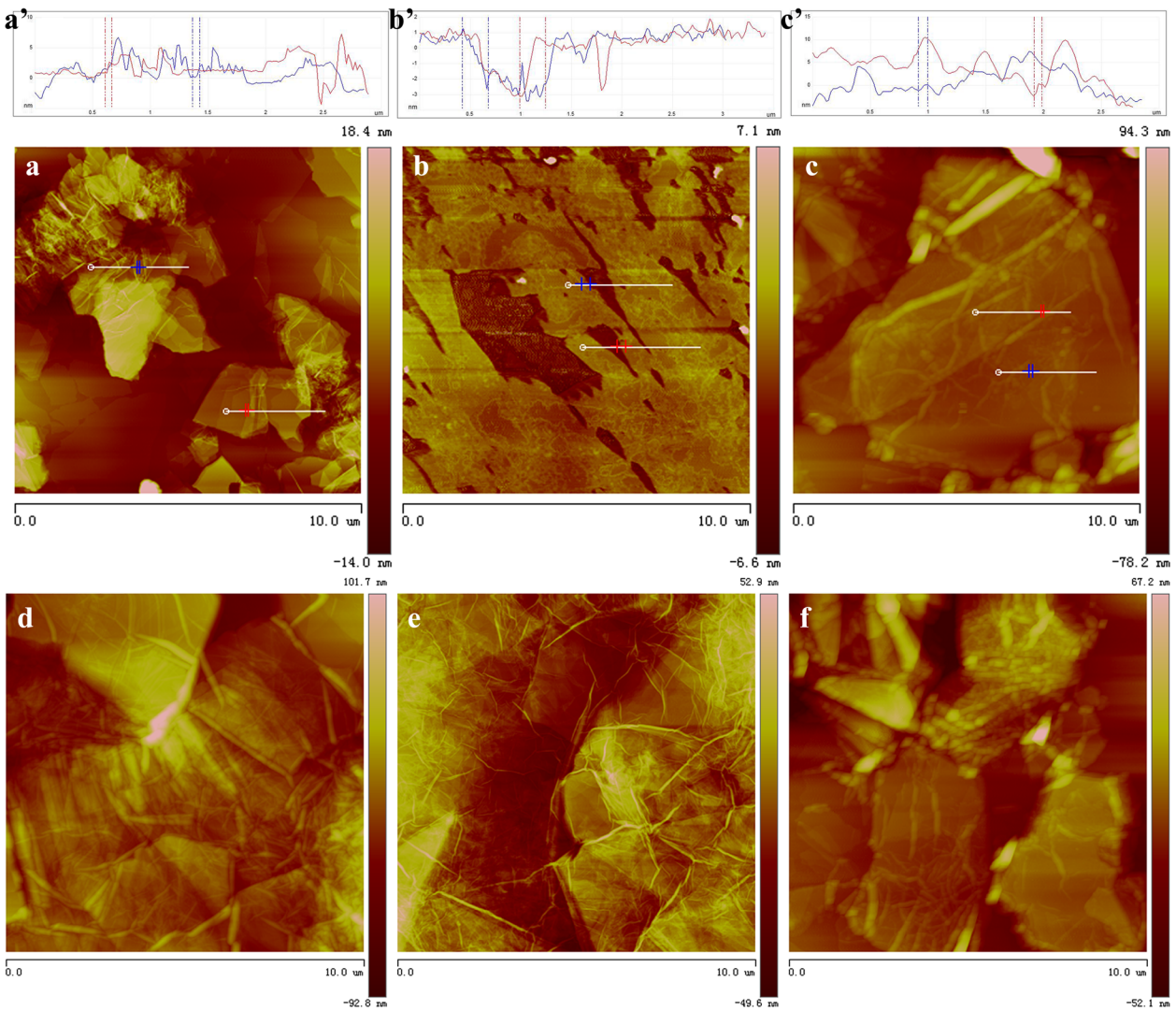

Fig. 3 AFM images with section analysis (**a**′–**c**′) of monolayer Langmuir films of GO-SH spread on pure water surface (**a**, **d**), DA subphase without UV light (**b**, **e**), and with UV light by interfacial thiol-ene photopolymerization (**c**, **f**). The transferred surface pressures are 5 mN/m for images (**a**–**c**) and 15 mN/m for images (**d**–**f**)

and some strip-like aggregates appear on GO sheet (Fig. 3c), suggesting the interfacial thiol-ene photopolymerization between thiol groups in GO-SH and DA molecules. In addition, with the increment of surface pressure of 15 mN/m, closely packed self-assembled films with obviously increased thickness can be formed, as shown in Fig. 3d–f. The difference of morphologies and height between the GO-SH Langmuir films from various subphases can be mainly due to the introduction of the DA molecules in the composite Langmuir film. In addition, we also compared the morphologies of multilayer LB films of GO-SH from pure water and DA subphase with UV light by thiol-ene photopolymerization. It is clearly observed from SEM images in Fig. 4 that the Langmuir films from pure water show dispersed GO-SH sheets, while the films from DA subphase by photopolymerization reaction demonstrate crosslinked films with embedded GO sheets.

It is well known that Raman spectroscopy has been widely applied to characterize GO and relative composite materials. The measurement for the present obtained multilayer LB films of GO-SH from pure water surface and DA subphase by in situ thiol-ene photopolymerization was performed. Two characteristic bands of graphene sheets in Raman spectra appear in Fig. 5a. One band at 1601 cm^{-1} can be assigned to the G band, which originates from the first-order scattering of the E_2g phonons of the sp^2-hybridized carbon atoms. Another band at 1351 cm^{-1} can be attributed to the D band, which comes from a breathing mode of κ-point phonons of

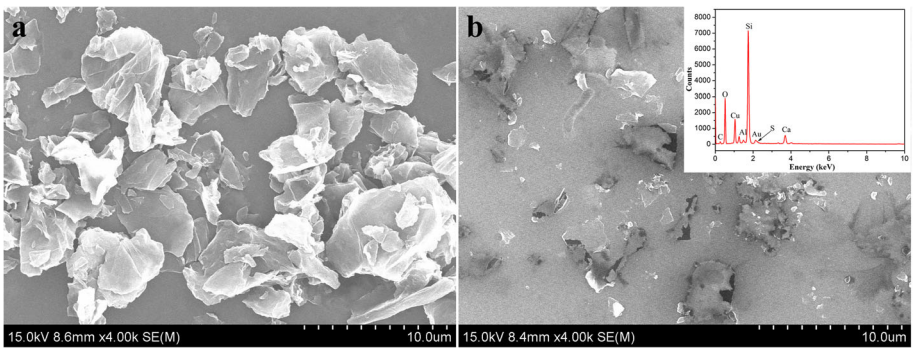

Fig. 4 SEM images with EDX spectra analysis of transferred 10-layered multilayer LB films of GO-SH from pure water surface (**a**) and DA subphase with UV light by interfacial thiol-ene photopolymerization (**b**)

A_1g symmetry of the defects involved in the sp^3-hybridized carbon bonds such as hydroxyl and/or epoxide bonds [51, 52]. It was reported that the D/G peak intensity ratio could be used as a measurement of the sp^2 domain size of graphene sheets containing sp^3 and sp^2 bonds due to the origination of G and D bands [53, 54]. For the present system in Fig. 5b, the D/G ratio shifted from 1.09 for LB films from water surface to 1.18 for LB films from DA subphase by in situ thiol-ene photopolymerization. The obvious change confirmed the successful photopolymerization reaction of polymeric DA molecules with thiol groups linked to GO sheet in the Langmuir films. In addition, the analysis of measured Raman spectra for the prepared GO-SH powder (Additional file 1: Figure S2) shows the calculated D/G ratio value of 1.05 in comparison with 0.91 and 0.92 for GO and GO–COOH materials.

To characterize the composition and chemical state of different LB films, we performed X-ray photoelectron spectroscopy (XPS) measurements (Fig. 6). The survey data for GO-SH LB films demonstrate the characteristic C(1s), O(1s), and S(2p) peaks (Fig. 6a). In addition, obvious $S(2p_{3/2})$ and $S(2p_{1/2})$ peaks appear at the center positions of 163.3 and 164.6 eV, respectively (Fig. 6b), which can be assigned to the dominant C–SH and small amount of C–S–C bond [55–57]. Thus the majority of sulfur element in LB films (about 83%) is displayed to be covalently attached to GO in thiol group. The deconvolution of C(1s) peaks from the films on pure water surface in Fig. 6c demonstrates the peaks centered at positions of 284.2, 285.1, 286.7, and 288.1 eV, which can be assigned to the C–C, C=C, and C–H bonds, C–N, C–O, and C=O–O oxygen-containing bonds, respectively [58–60]. After in situ thiol-ene photopolymerization, the deconvolution C(1s) peaks attributed to C–O and C=O–O bonds showed obvious increment (Fig. 6d). Moreover, according to the analysis data in Table 1, the N/C ratio and S/C ratio are calculated to decrease 25 and 51% after thiol-ene photopolymerization, indicating the addition of carbon element composition and successful preparation of GO-polymer composite Langmuir films. In addition, the survey XPS spectra of all as-prepared lyophilized (Additional file 1: Figure S3A) demonstrate the additional characteristic N(1s) and S(2p) peaks in GO-SH powder compared with spectra of GO and GO–COOH.

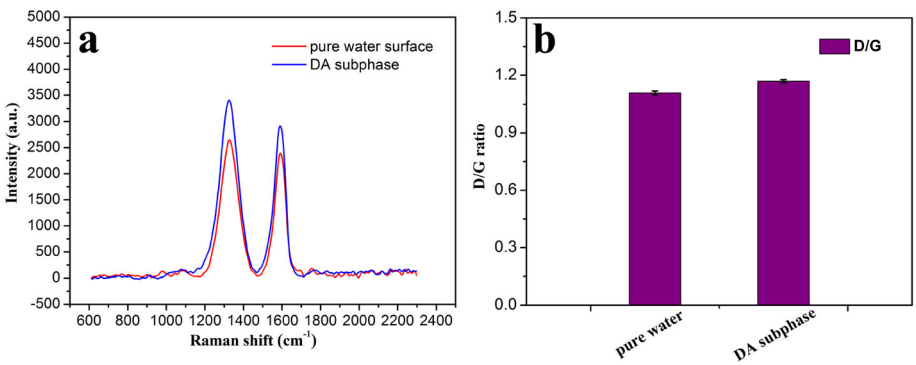

Fig. 5 Raman spectra (**a**) and D/G ratio analysis (**b**) of transferred 40-layered LB films of GO-SH from pure water surface and DA subphase by interfacial thiol-ene photopolymerization

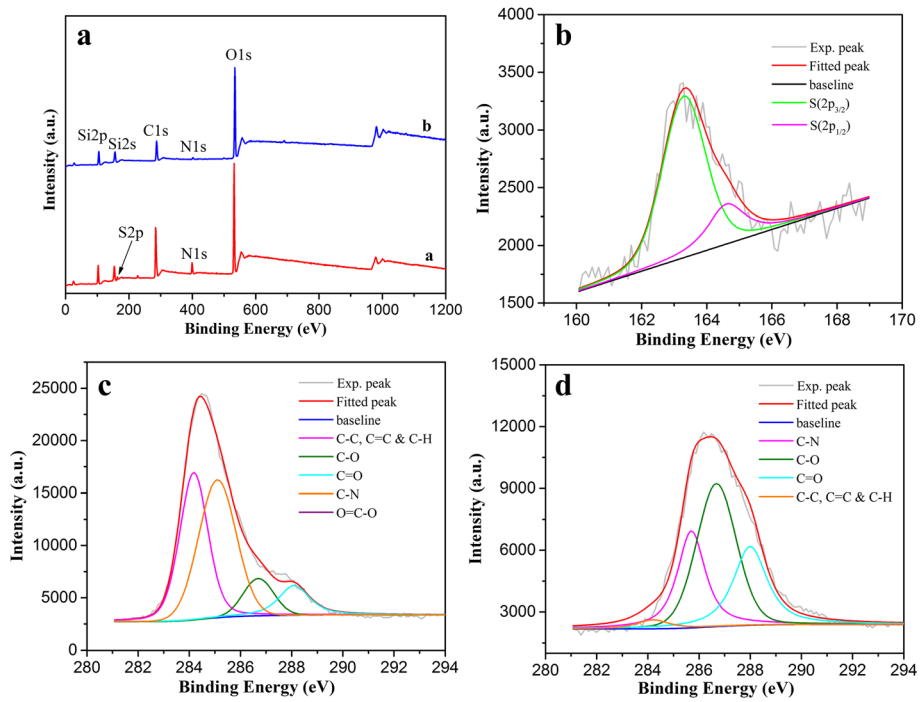

Fig. 6 Survey XPS spectra (A) of transferred 40-layered LB films of GO-SH on pure water surface (**a**) and DA subphase by interfacial thiol-ene photopolymerization (**b**). Deconvolution of XPS peaks of films on pure water surface (B, S(2p); C, C(1s)), and DA subphase by interfacial thiol-ene photopolymerization (D, C(1s))

The deconvolution analysis of C(1s) peaks in GO-SH (Additional file 1: Figure S3D) shows also the new peak centered at position of 285.2 eV assigned to the C–N bonds compared with those in GO and GO–COOH (Additional file 1: Figure S3B, C), which indicate the successful thiolation in GO sheets with cysteamine molecules.

In order to evaluate the successful functionalization in GO sheet and characterize the prepared composite films, FT-IR spectra were measured. The spectra of GO and GO–COOH in Additional file 1: Figure S4 show typical bands due to skeletal vibrations of graphene domains at 1632 cm^{-1} and characteristic OH and C=O stretching at 3432 and 1737 cm^{-1}, respectively [61–64]. As for spectrum of GO-SH, some new characteristic bands appeared, such as amide C=O stretching at 1640 cm^{-1}, N-H bending at 3312 cm^{-1} and N-H stretching at 1548 cm^{-1}, which indicated the effective functionalization of thiol groups. In addition, obvious changes were observed for the IR spectra of transferred multilayer LB films of GO-SH before and after thiol-ene photopolymerization with DA subphase (Additional file 1: Figure S5). The spectrum of GO-SH composite films after thiol-ene photopolymerization show obvious intensity increment for bands at 2921 and 2850 cm^{-1} (C–H modes of methylene moieties), 1727 cm^{-1} (C=O stretching), and 1640 cm^{-1} (amide C=O stretching), indicating the addition of cysteamine molecules in films and effective thiol-functionalization. Moreover, the measured XRD curves of multilayer LB films of GO-SH before and after thiol-ene photopolymerization reaction show similar broad Bragg peaks centered at 2θ value of 22.7° (Additional file 1: Figure S6), which suggest the retainment of 3D structures in composite films. Taken together, the supramolecular graphene oxide-polymer composite Langmuir films have been constructed by in situ thiol-ene photopolymerization, providing a potential for further application in GO functionalization and soft matter engineering.

Table 1 Analysis of XPS data of as-prepared multilayer GO-SH LB films from different subphase[a]

GO-SH LB Films	C [at.%]	N [at.%]	S [at.%]	N/C ratio [%]	S/C ratio [%]
Pure water	44.03	5.61	1.57	12.7	3.57
DA subphase with UV light	31.47	3.01	0.54	9.56	1.72

[a]Values calculated from integrated area in XPS data in Fig. 6

Conclusions

In summary, we have presented a one-step chemical preparation of graphene oxide-polymer composite Langmuir films by in situ thiol-ene photopolymerization reaction in a facile and effective manner. Thiol-

functionalized graphene oxide alone serves as either a crosslinking agent or an amphiphile for the formation of composite Langmuir films. The obtained GO-SH-DA composite films are demonstrated by the presence of a 3D nanostructure with embedded GO sheets in cross-linked films. The mechanism for the formation of the stable composite films involves a chemical thiol-ene photopolymerization reaction of thiol groups modified on GO sheet with ene components in soluble polymer chains. The resulting GO-polymer composite films can be easily transferred onto a supported substrate with assistance of the LB assembly method. Owing to the specific mechanical and chemical properties of graphene oxide and polymer composition, the present prepared composite films will have great potentials for application of soft matter engineering and graphene self-assembled nanomaterials.

Additional File

Additional file 1: Supporting information. (DOCX 5395 kb)

Acknowledgements
This work was financially supported by the National Natural Science Foundation of China (No. 21473153), the Support Program for the Top Young Talents of Hebei Province, the China Postdoctoral Science Foundation (No. 2015 M580214), the Scientific and Technological Research and Development Program of Qinhuangdao City (No. 201502A006), and the Open Funding Project of the National Key Laboratory of Biochemical Engineering (No. 2013KF-02).

Authors' Contributions
XL and KM contributed equally to this work. XL and KM participated in the analysis and the testing of the Langmuir films. RX and LZ carried out the synthesis and characterization of GO materials. TJ and BL supervised this work, helped in the analysis and interpretation of data, and, together with LZ, worked on the drafting and revisions of the manuscript. JZ conceived of the study and participated in its design and characterization. LZ and JZ participated in the design of the study and provided analysis instruments. All authors read and approved the final manuscript.

Authors' Information
XL, KM, and RX are PhD students. JZ is a research assistant. TJ, LZ, and BL are professors.

Competing Interests
The authors declare that they have no competing interests.

Author details
[1]State Key Laboratory of Metastable Materials Science and Technology, Yanshan University, Qinhuangdao 066004, People's Republic of China. [2]Hebei Key Laboratory of Applied Chemistry, School of Environmental and Chemical Engineering, Yanshan University, Qinhuangdao 066004, People's Republic of China. [3]Institute of Process Engineering, State Key Laboratory of Biochemical Engineering, Chinese Academy of Sciences, Beijing 100190, People's Republic of China. [4]Department of Chemistry and Biochemistry, Central Michigan University, Mount Pleasant, MI 48859, USA.

Received: 27 September 2016 Accepted: 25 January 2017
Published online: 08 February 2017

References
1. Li F, Jiang X, Zhao JJ, Zhang SB (2015) Graphene oxide: a promising nanomaterial for energy and environmental applications. Nano Energy 16:488–515
2. Zhang YY, Gong SS, Zhang Q, Ming P, Wan SJ, Peng JS, Jiang L, Cheng QF (2016) Graphene-based artificial nacre nanocomposites. Chem Soc Rev 45:2378–2395
3. Guo H, Jiao T, Zhang Q, Guo W, Peng Q, Yan X (2015) Preparation of graphene oxide-based hydrogels as efficient dye adsorbents for wastewater treatment. Nanoscale Res Lett 10:272
4. Yang W, Yang W, Ding F, Sang L, Ma Z, Shao G (2017) Template-free synthesis of ultrathin porous carbon shell with excellent conductivity for high-rate supercapacitors. Carbon 111:419–427
5. Narayan R, Kim SO (2015) Surfactant mediated liquid phase exfoliation of graphene. Nano Convergence 2:20
6. Ghosh D, Kim SO (2015) Chemically modified graphene based supercapacitors for flexible and miniature devices. Electron Mater Lett 11:719–734
7. Narayan R, Kim JE, Kim JY, Lee KE, Kim SO (2016) Graphene oxide liquid crystals: discovery, evolution and applications. Adv Mater 28:3045–3068
8. Oh Y, Le VD, Maiti UN, Hwang JO, Park WJ, Lim J, Lee KE, Bae YS, Kim YH, Kim SO (2015) Selective and regenerative carbon dioxide capture by highly polarizing porous carbon nitride. ACS Nano 9:9148–9157
9. Haq AU, Lim J, Yun JM, Lee WJ, Han TH, Kim SO (2013) Direct growth of polyaniline chains from N-doped sites of carbon nanotubes. Small 9:3829–3833
10. Shim J, Yun JM, Yun T, Kim P, Lee KE, Lee WJ, Ryoo R, Pine DJ, Yi GR, Kim SO (2014) Two-minute assembly of pristine large-area graphene based films. Nano Lett 14:1388–1393
11. Daud M, Kamal MS, Shehzad F, Al-Harthi MA (2016) Graphene/layered double hydroxides nanocomposites: a review of recent progress in synthesis and applications. Carbon 104:241–252
12. Jeong GH, Baek S, Lee S, Kim SW (2016) Metal oxide/graphene composites for supercapacitive electrode materials. Chem Asian J 11:949–964
13. Jiao T, Liu Y, Wu Y, Zhang Q, Yan X, Gao F, Bauer A, Liu J, Zeng T, Li B (2015) Facile and scalable preparation of graphene oxide-based magnetic hybrids for fast and highly efficient removal of organic dyes. Sci Rep-UK 5:12451
14. Texter J (2015) Graphene oxide and graphene flakes as stabilizers and dispersing aids. Curr Opin Colloid Interface Sci 20:454–464
15. Gambhir S, Jalili R, Officer DL, Wallace GG (2015) Chemically converted graphene: scalable chemistries to enable processing and fabrication. NPG Asia Mater 7, e186
16. Xing R, Jiao T, Liu Y, Ma K, Zou Q, Ma G, Yan X (2016) Co-assembly of graphene oxide and albumin/photosensitizer nanohybrids towards enhanced photodynamic therapy. Polymers-Basel 8:181
17. Niyogi S, Bekyarova E, Itkis ME, Mcwilliams JL, Hamon MA, Haddon RC (2006) Solution properties of graphite and graphene. J Am Chem Soc 128:7720–7721
18. Stankovich S, Piner RD, Nguyen SBT, Ruoff RS (2006) Synthesis and exfoliation of isocyanate-treated graphene oxide nanoplatelets. Carbon 44:3342–3347
19. Liu ZB, Xu YF, Zhang XY, Zhang XL, Chen YS, Tian JG (2009) Porphyrin and fullerene covalently functionalized graphene hybrid materials with large nonlinear optical properties. J Phys Chem B 113:9681–9686
20. Kaminska I, Barras A, Coffinier Y, Lisowski W, Niedziolka-Jonsson J, Woisel P, Lyskawa J, Opallo M, Siriwardena A, Boukherroub R, Szunerits S (2012) Preparation of a responsive carbohydrate-coated biointerface based on graphene/azido-terminated tetrathiafulvalene nanohybrid material. ACS Appl Mater Inter 4:5386–5393
21. Kaminska I, Das MR, Coffinier Y, Niedziolka-Jonsson J, Sobczak J, Woisel P, Lyskawa J, Opallo M, Boukherroub R, Szunerits S (2012) Reduction and functionalization of graphene oxide sheets using biomimetic dopamine derivatives in one step. ACS Appl Mater Inter 4:1016–1020
22. Yang YF, Wang J, Zhang J, Liu JC, Yang XL, Zhao HY (2009) Exfoliated graphite oxide decorated by PDMAEMA chains and polymer particles. Langmuir 25:11808–11814
23. Salavagione HJ, Gómez MA, Martínez G (2009) Polymeric modification of graphene through esterification of graphite oxide and poly (vinyl alcohol). Macromolecules 42:6331–6334
24. Lowe AB, Hoyle CE, Bowman CN (2010) Thiol-yne click chemistry: a powerful and versatile methodology for materials synthesis. J Mater Chem 20:4745–4750
25. Hoyle CE, Lowe AB, Bowman CN (2010) Thiol-click chemistry: a multifaceted toolbox for small molecule and polymer synthesis. Chem Soc Rev 39:1355–1387
26. Meziane D, Barras A, Kromka A, Houdkiva J, Boukherroub R, Szunerits S (2012) Thiol-yne reaction on boron-doped diamond electrodes: application for the electrochemical detection of DNA–DNA hybridization events. Anal Chem 84:194–200
27. Li HM, Cheng FO, Duft AM, Adronov A (2005) Functionalization of single-walled carbon nanotubes with well-defined polystyrene by "click" coupling. J Am Chem Soc 127:14518–14524

28. Kolb HC, Finn MG, Sharpless KB (2001) Click chemistry: diverse chemical function from a few good reactions. Angew Chem Int Ed 40:2004–2021
29. Salvio R, Krabbenborg S, Naber WJM, Velders AH, Reinhoudt DN, van der Wiel WG (2009) The formation of large-area conducting graphene-like platelets. Chem Eur J 15:8235–8240
30. Sun ST, Cao YW, Feng JC, Wu PY (2010) Click chemistry as a route for the immobilization of well-defined polystyrene onto graphene sheets. J Mater Chem 20:5605–5607
31. Kou L, He H, Gao C (2010) Click chemistry approach to functionalize two-dimensional macromolecules of graphene oxide nanosheets. Nano-Micro Lett 2:177–183
32. Kaminska I, Qi W, Barras A, Sobczak J, Niedziolka-Jonsson J, Woisel P, Lyskawa J, Laure W, Opallo M, Li M, Boukherroub R, Szunerits S (2013) Thiol–yne click reactions on alkynyl–dopamine-modified reduced graphene oxide. Chem Eur J 19:8673–8678
33. Gaines GL Jr (1966) Insoluble monolayers at liquid–gas interfaces. Wiley, New York
34. Ulman A (1991) An introduction to ultrathin organic films. Academic Press, New York
35. Roberts GG (1990) Langmuir–Blodgett films. Plenum, New York
36. Cote LJ, Kim F, Huang J (2009) Langmuir–Blodgett assembly of graphite oxide single layers. J Am Chem Soc 131:1043–1049
37. Kim F, Cote LJ, Huang J (2010) Graphene oxide: surface activity and two-dimensional assembly. Adv Mater 22:1954–1958
38. Jaafar MM, Ciniciato GPMK, Ibrahim SA, Phang SM, Yunus K, Fisher AC, Iwamoto M, Vengadesh P (2015) Preparation of a three-dimensional reduced graphene oxide film by using the Langmuir-Blodgett method. Langmuir 31:10426–10434
39. Harrison KL, Biedermann LB, Zavadil KR (2015) Mechanical properties Langmuir monolayers: article of water-assembled graphene oxide guiding controlled transfer. Langmuir 31:9825–9832
40. Han F, Yang SM, Jing WX, Jiang ZD, Liu H, Li L (2015) A study on near-UV blue photoluminescence in graphene oxide prepared by Langmuir-Blodgett method. Appl Surf Sci 345:18–23
41. Han TH (2015) Direct assembly of graphene oxide on flexible substrates for highly transparent electrodes via the Langmuir-Blodgett technique. J Nanosci Nanotechno 15:1191–1194
42. Mangadlao JD, Santos CM, Felipe MJL, de Leon ACC, Rodrigues DF, Advincula RC (2015) On the antibacterial mechanism of graphene oxide (GO) Langmuir-Blodgett films. Chem Commun 51:2886–2889
43. Gur B, Sinoforoglu M, Meral K (2015) Fabrication of morphology controlled graphene oxide-dye composite films at the air–water interface. RSC Adv 5:552–557
44. McGrail BT, Mangadlao JD, Rodier BJ, Swisher J, Advincula R, Pentzer E (2016) Selective mono-facial modification of graphene oxide nanosheets in suspension. Chem Commun 52:288–291
45. Wen J, Jiang Y, Yang Y, Li S (2014) Conducting polymer and reduced graphene oxide Langmuir–Blodgett films: a hybrid nanostructure for high performance electrode applications. J Mater Sci-Mater El 25:1063–1071
46. Singh BP, Nayak S, Nanda KK, Singh A, Takai C, Takashi S, Fuji M. Transparent, flexible, and conducting films based on graphene–polymer composites. Polym Compos. doi: 10.1002/pc.23935.
47. Li D, Muller MB, Gilje S, Kaner RB, Wallace GG (2008) Processable aqueous dispersions of graphene nanosheets. Nature Nanotechnol 3:101–105
48. Jeon SJ, Kwak SY, Yim D, Ju JM, Kim JH (2014) Chemically-modulated photoluminescence of graphene oxide for selective detection of neurotransmitter by "turn-on" response. J Am Chem Soc 136:10842–10845
49. Orth ES, Fonsaca JES, Domingues SH, Mehl H, Oliveira MM, Zarbin AJG (2013) Targeted thiolation of graphene oxide and its utilization as precursor for graphene/silver nanoparticles composites. Carbon 61:543–550
50. Chen G, Zhai S, Zhai Y, Zhang K, Yue Q, Wang L, Zhao J, Wang H, Liu J, Jia J (2011) Preparation of sulfonic-functionalized graphene oxide as ion-exchange material and its application into electrochemiluminescence analysis. Biosens Bioelectron 26:3136–3141
51. Ferrari AC, Robertson J (2000) Interpretation of Raman spectra of disordered and amorphous carbon. Phys Rev B 61:14095–14107
52. Malard LM, Pimenta MA, Dresselhaus G, Dresselhaus MS (2009) Raman spectroscopy in graphene. Phys Rep 473:51–87
53. Kudin KN, Ozbas B, Schniepp HC, Prudhomme RK, Aksay IA, Car R (2008) Raman spectra of graphite oxide and functionalized graphene sheets. Nano Lett 8:36–41
54. Kim KS, Zhao Y, Jang H, Lee SY, Kim JM, Kim KS, Ahn JH, Kim P, Choi JY, Hong BH (2009) Large-scale pattern growth of graphene films for stretchable transparent electrodes. Nature 457:706–710
55. Lindberg BJ, Hamrin K, Johansson G, Gelius U, Fahlman A, Nordling C, Siegbahn K (1970) Molecular spectroscopy by means of ESCA II. Sulfur compounds. Correlation of electron binding energy with structure. Phys Scr 1:286
56. Thomas HR, Marsden AJ, Walker M, Wilson NR, Rourke JP (2014) Sulfur-functionalized graphene oxide by epoxide ring-opening. Angew Chem Int Ed 53:7613–7618
57. Chen X, Dai YC, Zheng ZB, Wang KZ (2013) Photoelectrochemical properties of electrostatically self-assembled multilayer films formed by a cobalt complex and graphene oxide. J Colloid Interface Sci 402:107–113
58. Akhavan O (2015) Bacteriorhodopsin as a superior substitute for hydrazine in chemical reduction of single-layer graphene oxide sheets. Carbon 81:158–166
59. Xing R, Liu K, Jiao T, Zhang N, Ma K, Zhang R, Zou Q, Ma G, Yan X (2016) An injectable self-assembling collagen-gold hybrid hydrogel for combinatorial antitumor photothermal/photodynamic therapy. Adv Mater 28:3669–3676
60. Ma ZP, Shao GJ, Fan YQ, Wang GL, Song JJ, Shen DJ (2016) Construction of hierarchical alpha-MnO_2 nanowires@ultrathin delta-MnO_2 nanosheets core-shell nanostructure with excellent cycling stability for high-power asymmetric supercapacitor electrodes. ACS Appl Mater Inter 8:9050–9058
61. Grayfer ED, Nazarov AS, Makotchenko VG, Kim SJ, Fedorov VE (2011) Chemically modified graphene sheets by functionalization of highly exfoliated graphite. J Mater Chem 21:3410–3414
62. Zhang R, Xing R, Jiao T, Ma K, Chen C, Ma G, Yan X (2016) Carrier-free, chemo-photodynamic dual nanodrugs via self-assembly for synergistic antitumor therapy. ACS Appl Mater Inter 8:13262–13269
63. Ma K, Xing R, Jiao T, Shen G, Chen C, Li J, Yan X (2016) Injectable self-assembled dipeptide-based nanocarriers for tumor delivery and effective in vivo photodynamic therapy. ACS Appl Mater Inter 8:30759–30767
64. Bao Q, Zhang D, Qi P (2011) Synthesis and characterization of silver nanoparticle and graphene oxide nanosheet composites as a bactericidal agent for water disinfection. J Colloid Interface Sci 360:463–470